Triptolide attenuates cardiac remodeling by inhibiting pyroptosis and EndMT via modulating USP14/Keap1/Nrf2 pathway

Lina Ba [a,b,1], Mingyao E [b,c,1], Ruixuan Wang [b], Nan Wu [b], Rui Wang [b], Renling Liu [b], Xiang Feng [b], Hanping Qi [b], Hongli Sun [b], Guofen Qiao [a,*]

[a] *Department of Pharmacology, State-Province Key Laboratories of Biomedicine-Pharmaceutics of China, Key Laboratory of Cardiovascular Medicine Research, Ministry of Education, College of Pharmacy, Harbin Medical University, Harbin, 150081, China*
[b] *Department of Pharmacology, Harbin Medical University-Daqing, Daqing, Heilongjiang, 163319, China*
[c] *Key Laboratory of Bio-Macromolecules of Chinese Medicine, Changchun University of Chinese Medicine, Changchun, 130117, China*

ABSTRACT

Background: Cardiac remodeling is a common pathological feature in many cardiac diseases, characterized by cardiac hypertrophy and fibrosis. Triptolide (TP) is a natural compound derived from Tripterygium wilfordii Hook F. However, the related mechanism of it in cardiac remodeling has not been fully understood.
Methods and results: Transverse aortic constriction (TAC)-induced cardiac hypertrophic mouse model and angiotensin II (Ang II)-induced cardiomyocytes hypertrophic model were performed. Firstly, the results indicate that TP can improve cardiac function, decreased cardiomyocyte surface area and fibrosis area, as well as lowered the protein expressions of brain natriuretic peptide (BNP), β-major histocompatibility complex (β-MHC), type I and III collagen (Col I and III). Secondly, TP suppressed cardiac pyroptosis, and decreased the levels of Interleukin-1β (IL-1β), Interleukin-18 (IL-18) by Enzyme-linked immunosorbent assay (ELISA), and pyroptosis-associated proteins. Furthermore, TP enhanced the expressions of Nuclear factor erythroid 2-related factor 2 (Nrf2) and Heme oxygenase 1 (HO-1). Interestingly, when Nrf2 was silenced by siRNA, TP lost its properties of reducing pyroptosis and cardiac hypertrophy. In addition, in the Transforming Growth Factor β1 (TGF-β1)-induced primary human coronary artery endothelial cells (HCAEC) model, TP was found to inhibit the process of endothelial-to-mesenchymal transition (EndMT), characterized by the loss of endothelial-specific markers and the gain of mesenchymal markers. This was accompanied by a suppression of Slug, Snail, and Twist expression. Meanwhile, the inhibitory effect of TP on EndMT was weakened when Nrf2 was silenced by siRNA. Lastly, potential targets of TP were identified through network pharmacology analysis, and found that Ubiquitin-Specific Protease 14 (USP14) was one of them. Simultaneously, the data indicated that decrease the upregulation of USP14 and Kelch-like ECH-Associated Protein 1 (Keap1) caused by cardiac remodeling. However, Keap1 was decreased and Nrf2 was increased when USP14 was silenced. Furthermore, CoIP analysis showed that USP14 directly interacts with Keap1.
Conclusion: TP can observably reduce pyroptosis and EndMT by targeting the USP14/Keap1/Nrf2 pathway, thereby significantly attenuating cardiac remodeling.

---

* Corresponding author.
  E-mail address: qiaogf@hrbmu.edu.cn (G. Qiao).
[1] These authors contributed equally to this work and share first authorship.

1. Introduction

Cardiac remodeling is characterized by the hypertrophy of cardiomyocytes (CM), CM death, activation of cardiac fibroblasts (CF), and deposition of extracellular matrix (ECM), as a response to risk factors such as hypertension and coronary artery disease [1,2]. Initially, cardiac hypertrophy and fibrosis can compensate for a while and improve cardiac function [3]. However, sustained hypertrophy and fibrosis can cause the ventricles to dilate, leading to insufficient pump function and diastolic dysfunction, ultimately resulting in heart failure (HF), which is a significant determinant of clinical outcomes [4]. Currently, there are no specific treatments for cardiac remodeling in patients, and clinical therapeutics mainly involve lowering cardiac pressure, or reducing volume overload, and preventing adrenergic receptors [5]. Therefore, effective therapy that could prevent cardiac remodeling is crucial.

Triptolide (TP), a bioactive epoxy-2-terpenoid ester compound isolated from the traditional Chinese medicine Tripterygium wilfordii Hook F., has been used for treating various diseases for over a hundred years [6,7]. Its beneficial physiological properties have been demonstrated in different areas, such as anti-tumor [8,9], anti-inflammatory [10,11], and immunomodulatory [12] effects. Meanwhile, TP could attenuate subretinal fibrosis by suppressing TGF-β1 induced epithelial–mesenchymal transition (EMT) [13]. Accumulated evidence suggests that TP also has a protective effect on cardiovascular diseases. Yang et al. and Xi et al. have shown that TP could inhibit ischemia/reperfusion injury and glucose uptake via the inhibition of Reactive Oxygen Species (ROS) and IKKβ–NF–κB pathway in CM, respectively [14,15]. Moreover, Pan et al. have reported that TP could effectively alleviate cardiac remodeling by activating FoxP3 to inhibit mitophagy [16]. However, the precise mechanisms of TP on cardiac remodeling remain to be fully understood.

Pyroptosis is a type of programmed cell death accompanied by the release of pro-inflammatory cytokines [17]. This process has been implicated in the pathogenesis of various diseases, such as liver injury [18], acute lung injury [19], and tumors [20]. Recently, mounting evidence suggests that pyroptosis also plays a pivotal role in cardiac diseases. Excessive pyroptosis can cause cardiac hypertrophy, cardiomyocytes death, myocardial dysfunction, excessive inflammation and promote cardiac remodeling [21]. Meanwhile, Pyroptosis in cardiomyocytes are essential for myocardial fibrosis in response to pressure overload in the early stages of chronic heart failure [22]. Lei et al. have demonstrated that inhibiting pyroptosis in CM could alleviate myocardial ischemia/reperfusion injury [23]. Importantly, Wang et al. and Yue et al. have found that controlling cardiomyocyte pyroptosis could prevent cardiac hypertrophy [24, 25]. However, few studies have focused on the role of TP in the pyroptosis of cardiac hypertrophy.

Endothelial-to-mesenchymal transition (EndMT) is a dynamic process characterized by the down-regulation of endothelial-specific markers such as VE-cadherin and Platelet Endothelial Cell Adhesion Molecule 1 (CD31), increased cell migration, and up-regulation of mesenchymal-specific markers such as α-smooth muscle actin (α-SMA) in endothelial cells, resulting in the expression of transcriptional factors expression including Snail, Slug and Twist [26,27]. Recently, EndMT has been increasingly recognized as an important process leading to various cardiovascular diseases in adults, including cardiac remodeling, atherosclerosis, cardiac fibrosis, and myocardial infarction [28–31]. EndMT has been reported to promote cardiac fibrosis, with quantitative lineage analysis showing that 27–35 % of fibroblasts in fibrotic heart tissue are derived from endothelial cells [30]. Numerous studies have shown that EndMT contributes significantly to TAC-induced cardiac fibrosis, and inhibiting EndMT has been demonstrated to attenuate cardiac fibrosis after TAC [32–34].

The objective of this study is to examine the potential cardioprotective effect of TP on cardiac remodeling induced by pressure overload. Further, our aim is to investigate whether TP can inhibit pyroptosis and EndMT, and to explore the underlying mechanisms involved.

2. Materials and methods

2.1. Animal and drug

All animal experiments in this study were approved by the Ethics Committee of Harbin Medical University (Daqing). Male C57BL/6J mice (8–10 weeks old, 22–25 g) were obtained from the animal center of Harbin Medical University. TP, obtained from Aladdin (Shanghai, China; purity≥98 % by high-performance liquid chromatography [HPLC]), was first dissolved in dimethyl sulfoxide (DMSO) and then diluted in saline to a final concentration of 0.1 % DMSO.

2.2. Surgical procedures and TP treatment

Mice underwent TAC surgery, as previously described [35]. Briefly, mice were intraperitoneally injected with 2 % pentobarbital sodium (40 mg/kg) and placed on mechanical ventilation. The aortic constriction was performed by ligating the transverse thoracic aorta with a 28-gauge needle and a 7-0 braided polyester suture. After 4 weeks, the hearts and tibias were harvested and weighed, and the heart weight/tibia length (HW/TL, mg/mm) and heart weight/body weight (HW/BW, mg/g) ratios were calculated and compared. The mouse was divided into 6 groups randomly. The groups were named as follows: (1) Sham; (2) Sham + triptolide (Sham + TP): mice were treated with TP (90 μg/kg/d); (3) TAC; (4) TAC + TP (TAC + TP-10): mice were treated with TP (10 μg/kg/d) after TAC; (5) TAC + TP (TAC + TP-30): mice were treated with TP (30 μg/kg/d) after TAC; (6) TAC + TP (TAC + TP-90): mice were treated with TP (90 μg/kg/d) after TAC. TP was administered intraperitoneally injection for 4 weeks.

2.3. Echocardiographic studies

4 weeks after TAC, the mice were anesthetized with isoflurane to undergo transthoracic echocardiographic examination, and the parameters were measured.

2.4. Histopathological studies

Firstly, the heart of the mouse was positioned in a 4 % paraformaldehyde solution at 4 °C overnight, and then a 30 % sucrose solution was placed. When the tissue sunk to the bottom of the 30 % sucrose solution, it was taken out and embedded in optimal cutting temperature compound (OCT) freezing medium and frozen at −20 °C. Use a microtome to knife the tissue into sections with a thickness of several microns and transfer to 3-aminopropyl triethoxysilane-coated slides. These sections were stained with haematoxylin-eosin (HE), Masson's trichrome and the histopathological changes were observed under the light microscope.

2.5. Western blotting

Total protein samples were extracted from tissues or cells using the same procedure previously described [36]. Briefly, heart tissues or cardiomyocytes were lysed by RIPA buffer. After centrifugation, the supernatant was collected. Protein extracts were mixed with SDS-PAGE. After electrophoresis, the protein transferred onto a nitrocellulose membrane. Then, the membranes were blocked and incubated with the primary antibodies: BNP (1:1000, ABclonal, China), β-MHC (1:1000, ABclonal, China), Caspase-1 (1:1000, GeneTex, USA), Nrf2 (1:1000, Proteintech, China) , HO-1 (1:1000, Wanleibio, China) , NLRP3 (1:1000, ABclonal, China) , Gasdermin-D (ABclonal, China), USP14 (1:1000, Proteintech, China), Snail (1:1000, Proteintech, China) , Twist (1:1000, Proteintech, China) , Slug (1:1000, ABclonal, China), CD31 (1:1000, ABclonal, China), VE-cadherin (1:1000, ABclonal, China), α-SMA (1:1000, BOSTER, China), Keap1 (1:1000, Proteintech, China), type I collagen (1:1000, ABclonal, China), type III collagen (1:1000, affinity, USA).

2.6. Enzyme linked immunosorbent assay (ELISA) studies

The concentrations of Interleukin 1β (IL-1β) and Interleukin 18 (IL-18) of arterial blood serum and cardiomyocytes were measured using commercially available ELISA kit (R&D system), according to the manufacturer's instructions, respectively.

2.7. Culture of cells

Mouse Cardiac Muscle Cell Line (HL-1) was purchased from iCell (China). HL-1 was cultured in MEM with 10 % fetal bovine serum and 1 % penicillin-streptomycin. Ang II was used to build cardiomyocytes hypertrophy model *in vitro*. In our study, HL-1 was incubated with 100 nmol/L Ang II for 48 h at 37 °C in a humidified incubator with 5 % CO_2. Cells were divided into 4 groups: (1) Control (Ctl); (2) Control + triptolide (Ctl + TP): cells were treated with triptolide (10 μg/L, 48 h); (3) Ang II: cells were treated with 100 nmol/L Ang II (48 h); (4) Ang II + triptolide (Ang II + TP): cells were exposed to 100 nmol/L Ang II and treated with triptolide (10 μg/L, 48h).

Primary human coronary artery endothelial cells (HCAEC) were purchased from Sciencell (U.S.A.). HCAEC were cultured with Endothelial Cell Medium (Sciencell U.S.A.) in a humid environment at 37 °C, 5 % CO_2. TGF-β1 was used to build HCAEC EndMT model *in vitro*. In our study, recombinant human TGF-β1 (10 ng/ml, MCE) was added to stimulate the cells for 6d to induce EndMT. Cells were divided into 4 groups: (1) Control (Ctl); (2) Control + triptolide (Ctl + TP): cells were treated with triptolide (10 μg/L); (3) TGF-β1: cells were treated with 10 ng/ml TGF-β1; (4) TGF-β1+ triptolide (TGF-β1+TP): cells were exposed to 10 ng/L TGF-β1 and treated with triptolide (10 μg/L).

## 2.8. Small interfering RNA (siRNA) transfection

Cardiomyocytes and HCAEC were transfected with siRNA-Nrf2, siRNA-USP14 or siRNA-Negative control (scRNA), which was purchased from GenePharma Co., Ltd. (Shanghai, China) using the X-treme GENE small interfering RNA (siRNA) transfection reagent (Roche) according to the manufacturer's protocol.

2.9. Terminal deoxynucleotidyl transferase dUTP nick end labeling (TUNEL)

According to the manufacturer's instructions, an in situ cell death detection kit (Roche, USA) was used to detect DNA fragmentation of individual cells in heart tissue sections. TUNEL staining was assessed via fluorescence microscopy (Leica, Germany).

2.10. PI/Hoechst 33342 staining assay

Following the proper treatment, the cells were stained with Hoechst 33342 and PI (Beyotime, China) for 10 min. The cells were observed using a fluorescence microscope (Leica, Germany).
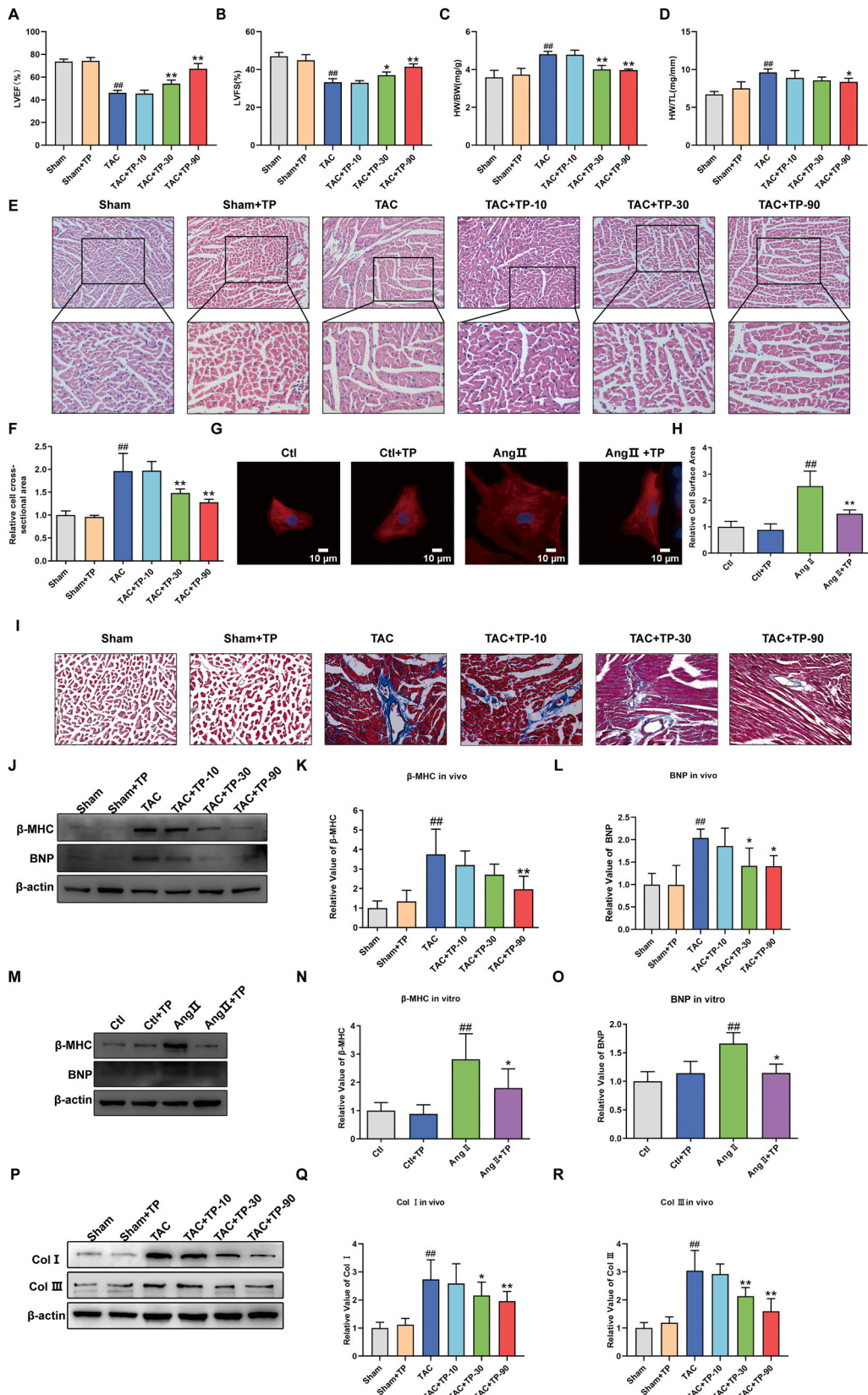
(caption on next page)

Fig. 1. TP alleviates cardiac remodeling *in vivo* and *in vitro*. (A–B) LVEF and LVFS measured by echocardiographic examination ($n = 6$). **(C–D)** Quantitative data of HW/BW and HW/TL ($n = 6$). **(E–F)** Representative images of HE staining of heart tissue, and quantification of cell cross-sectional area of cardiomyocytes ($n = 3$). **(G)** Representative immunofluorescent staining of the cardiomyocytes (HL-1, α-actinin, red) and nuclei (DAPI, blue) following AngII treatment, Scale bar: 10 μm. **(H)** Relative surface area of HL-1($n = 6$). **(I)** Representative images of Masson's trichrome staining of heart tissue, $n = 3$. **(J–L)** Cardiac hypertrophic marker protein β-MHC and BNP expression were measured in mouse heart tissue ($n = 6$). **(M–O)** Cardiac hypertrophic marker protein β-MHC and BNP expression were detected in HL-1 cardiomyocytes (n = 6). **(P–R)** Cardiac fibrotic marker protein Col I and III expression were measured in mouse heart tissue ($n = 6$). All the values are presented as mean ± SD. $^{\#}$P < 0.05, $^{\#\#}$P < 0.01 compared with Sham or Ctl group; *P < 0.05, **P < 0.01 compared with TAC or Ang II group. LVEF = Left ventricular ejection fraction; LVFS = Left ventricular fraction shortening; HW/BW=Heart weight to body weight ratio; HW/TL = Heart weight to tibia length ratio. The original blots were provided in supplementary data as Supplementary Fig. S1.

2.11. Immunofluorescence staining

The expression of sarcomeric α-actinin (α-SMA, BOSTER, China) protein in cardiomyocytes was performed by immunofluorescence staining. In detail, cells are fixed with 4 % paraformaldehyde, and then permeabilized in 0.2 % TritonX-100. Subsequently, the cells were incubated with α-SMA (1:200) overnight at 4 °C, after adding goat serum for 30min at room temperature. Then, the secondary antibody (1:200) was utilized to probe target proteins. DAPI was used to stain the cell nucleus of cardiomyocytes. Immunofluorescence was examined under a fluorescence microscope (Leica, Germany).

2.12. Co-immunoprecipitation (CoIP)

CoIP assays were performed according to the manufacturer's protocol (Thermo scientific co-ip (Pierce™ CO-Immunoprecipitation kit), USA). Immunoprecipitation complexes were analyzed by Western blotting.

2.13. Statistical analyses

Quantitative data were presented as the Mean ± Standard deviation (SD) and analyzed by SPSS20.0. Statistical differences were determined using two-tailed unpaired Student's t-tests or one-way analysis of variance (ANOVA) followed by Tukey's post-hoc analysis. Statistical significance was regarded as P < 0.05.

3. Results

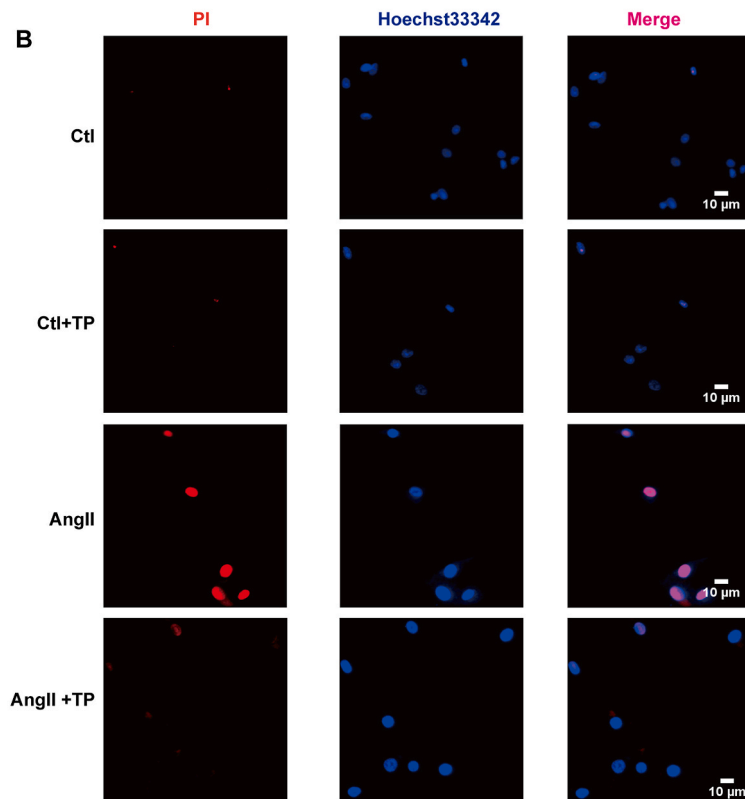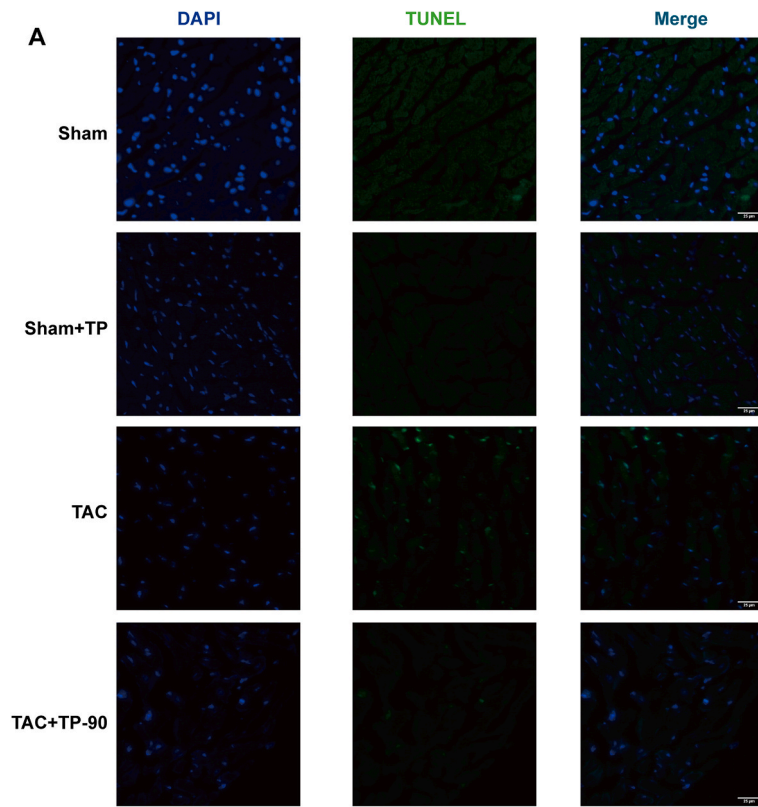### 3.1. TP alleviates cardiac remodeling in vivo and in vitro

In order to investigate the potential of TP to inhibit TAC-induced cardiac remodeling, echocardiographic examination was conducted. As illustrated in Fig. 1A–B, the results from echocardiographic examination revealed a significant decrease in the LVEF and LVFS in the TAC group compared to the Sham group. However, treatment with TP (30, 90 μg/kg) over a 4-week period was found to reverse these effects. Additionally, the morphological results indicated a notable decline in the HW/BW and HW/TL ratios in the TAC + TP-90 group compared to the TAC group (Fig. 1C–D). Moreover, both HE and immunofluorescence staining results demonstrated a reduction in the cell cross-sectional area (Fig. 1E–F) and mouse cardiomyocytes surface area (Fig. 1G–H) due to the administration of TP, compared to the TAC group and Ang II group respectively. Furthermore, results from Masson's trichrome staining demonstrated a significant increase in interstitial fibrotic areas in the remodeling heart compared to the Sham group. However, administration of TP was found to significantly reduce the extracellular matrix deposition in the remodeling heart (Fig. 1 I).

In addition, the protein expressions of cardiac hypertrophic and fibrotic markers, such as BNP, β-MHC, and Col I and III, were assessed. The results indicated that TP significantly reduced the levels of BNP and β-MHC *in vivo* (Fig. 1J-L) and *in vitro* (Fig. 1M−O) as well as decreased the expression of Col I and III *in vivo* (Fig. 1P–R). Thus, these findings suggest that TP effectively improves cardiac function and exhibits anti-myocardial hypertrophy and anti-myocardial fibrosis effects.

3.2. TP inhibits pyroptosis in cardiac remodeling models

Excessive cardiomyocyte pyroptosis has been shown to contribute to cardiac remodeling [21]. NLRP3 can convert precursor Caspase-1 to cleaved Caspase-1, which then cleaves IL-1β and IL-18 into their active forms. These cytokines initiate inflammatory responses that promote pyroptosis. Furthermore, GSDMD can be activated by Caspase-1, resulting in the release of its N-terminal domain, which oligomerizes on the membrane to form macropores. This ultimately causes the rupture of the membrane and cell death [37].

To further understand the inhibitory effect of TP on cardiac remodeling and its association with pyroptosis, pyroptosis-related proteins and factors were evaluated. As displayed in Fig. 2A–B, the results of the TUNEL test and Hoechst/PI staining showed that TAC or Ang II significantly increased the number of positive cells of pyroptosis, while TP was found to reverse this effect. Additionally, ELISA analysis demonstrated that TP visibly reduced the levels of IL-1β and IL-18 in the serum and in mouse cardiomyocytes (Fig. 3A–D). Furthermore, pyroptosis-related proteins, including NLRP3, cleaved-Caspase-1, and Gasdermin D (GSDMD), were measured. As expected, these protein expressions were reduced following TP treatment in heart tissue (Fig. 3E–H) and in mouse

A

DAPI TUNEL Merge

Sham

Sham+TP

TAC

TAC+TP-90

B

PI Hoechst33342 Merge

Ctl

Ctl+TP

AngII

AngII +TP

(caption on next page)

Fig. 2. TP exerted the inhibitory effects of on pyroptosis *in vivo* and *in vitro*. (A) Representative TUNEL staining in tissue slices of mouse heart tissue, scale bar: 25 μm. **(B)** Representative PI/Hoechst 33342 double staining in HL-1 cardiomyocytes, PI-positive cell (Red), Hoechst 33342 -positive cell (Blue), scale bar: 10 μm.

cardiomyocytes (Fig. 3I-L). Overall, these results suggest that TP is capable of suppressing cardiac remodeling by inhibiting excessive cardiomyocyte pyroptosis.

3.3. TP suppresses pyroptosis via activating Nrf2/HO-1 pathway

To investigate the potential signal pathways involved in the inhibitory effect of TP against pyroptosis in cardiac remodeling, the levels of Nrf2/HO-1 pathway proteins were measured. Western blotting analysis revealed that the expressions of Nrf2 and HO-1 were significantly down-regulated in cardiac remodeling models (Fig. 4A–F). However, after treatment with TP, these expressions were remarkably up-regulated. These results suggest that the inhibitory effect of TP in pyroptosis may involve the activation of the Nrf2/HO-1 signaling pathway.

To further confirm the inhibitory effect of TP on mouse cardiomyocyte pyroptosis via the Nrf2/HO-1 signaling pathway, Nrf2 was silenced in mouse cardiomyocytes by transfection with siRNA-Nrf2. The expression levels of Nrf2 and HO-1 were identified by Western blot. It was found that these protein expressions were significantly reduced by siRNA mixtures (Fig. 4G–J), indicating that the Nrf2 protein was successfully silenced.

ELISA assays showed that IL-1β and IL-18 were still present at high levels in the Ang II + TP + siRNA group, compared with the Ang II + TP + scRNA group (Fig. 4K-L). Furthermore, the protein expressions of NLRP3, cleaved-Caspase-1, and GSDMD following trip-tolide treatment were reversed by siRNA-Nrf2 (Fig. 4M−P). These findings suggest that TP inhibited pyroptosis via activating the Nrf2/HO-1 signaling pathway in the cardiac remodeling model.

To further determine the role of the Nrf2/HO-1 signaling pathway in the anti-hypertrophic effects of TP, the surface area of mouse cardiomyocytes and the protein levels of cardiac hypertrophy markers were evaluated. Immunofluorescence results showed that Nrf2 knockdown eliminated the inhibitory effect of TP on Ang II-induced enlarged cardiomyocytes (Fig. 4Q–R). Additionally, Western blotting data demonstrated that the ability of TP to inhibit the expression of cardiac hypertrophy markers, BNP and β-MHC, was significantly weakened by Nrf2 knockdown in Ang II-induced mouse cardiomyocytes (Fig. 4S-U). These data indicate that TP can alleviate cardiac hypertrophy, at least in part, through the Nrf2/HO-1 signaling pathway.

3.4. TP inhibits EndMT in cardiac remodeling models

Recent studies have shown that EndMT-derived CFs play an essential role in the pressure overload-induced cardiac fibrosis model [29,32]. During EndMT, endothelial cells lose their features such as CD31 and VE-Cadherin expressions and acquire mesenchymal features such as α-SMA expression. To assess the inhibitory effect of TP on EndMT in TAC mice, Western blotting assays of CD31, VE-Cadherin, and α-SMA were performed. The data showed that CD31 and VE-Cadherin were significantly down-regulated in the TAC group, and this down-regulation was reversed by TP treatment. In contrast, α-SMA was up-regulated in the TAC group, but this up-regulation was also reversed by TP treatment (Fig. 5A–D).

The EndMT process is also assessed by evaluating the expression of endothelial cell markers CD31 and VE-Cadherin and the mesenchymal marker α-SMA in HCAECs. The reduction of CD31 and VE-Cadherin and the increase of α-SMA were observed in the TGFβ1-induced transition (Fig. 5I-L). However, this phenomenon was attenuated after incubation with TP. These findings suggest that TP may inhibit EndMT in cardiac remodeling and thereby alleviate cardiac fibrosis.

Based on the results described above, it is demonstrated that TP can regulate the EndMT process. Several EndMT-promoting transcription factors, including Snail, Slug, and Twist, have been implicated in EndMT [38]. The data performed that TP can reverse the increase in Snail, Slug, and Twist protein expressions induced by TGF-β1 stimulation *in vivo* (Fig. 5E–H) and *in vitro* (Fig. 5M − P). These findings suggest that TP affects the EndMT process by regulating the expressions of EndMT-promoting tran-scription factors.

3.5. TP inhibits EndMT via Nrf2 pathway

Accumulated evidence suggests that the Nrf2 pathway is involved in the regulation of EndMT [39]. To investigate the molecular mechanism underlying the inhibitory effect of TP on the EndMT process, the activity of Nrf2 were assessed in endothelial cells. After TP treatment, Nrf2 was observed to be increased in TGFβ1-incubated endothelial cells (Fig. 6A–B). Consistent with the activation of Nrf2, TP potently increased the expression of EndMT-promoting transcription factors, including Snail, Slug, and Twist (Fig. 5M − P). These results indicate that TP activates the Nrf2 pathway, which may contribute to its inhibitory effect on the EndMT process.

To further confirm the role of the Nrf2 pathway in the inhibitory effect of TP on the EndMT process, siRNA technique to silence Nrf2 was used (Fig. 6C–D). Endothelial cells were transfected with Nrf2 siRNA before TGF-β1 treatment, and the levels of EndMT-related proteins were assessed by Western blotting. As depicted in Fig. 6E-H, when Nrf2 was inhibited, TGF-β1-induced EndMT was aggra-vated, which was accompanied by up-regulation of mesenchymal cell markers, such as α-SMA, and down-regulation of endothelial markers, including CD31 and VE-cadherin. Additionally, the level of EndMT-promoting transcription factors, such as Snail, Twist, and Slug, was increased by Nrf2 siRNA transfection in endothelial cells treated with TGF-β1, as compared to scramble siRNA control
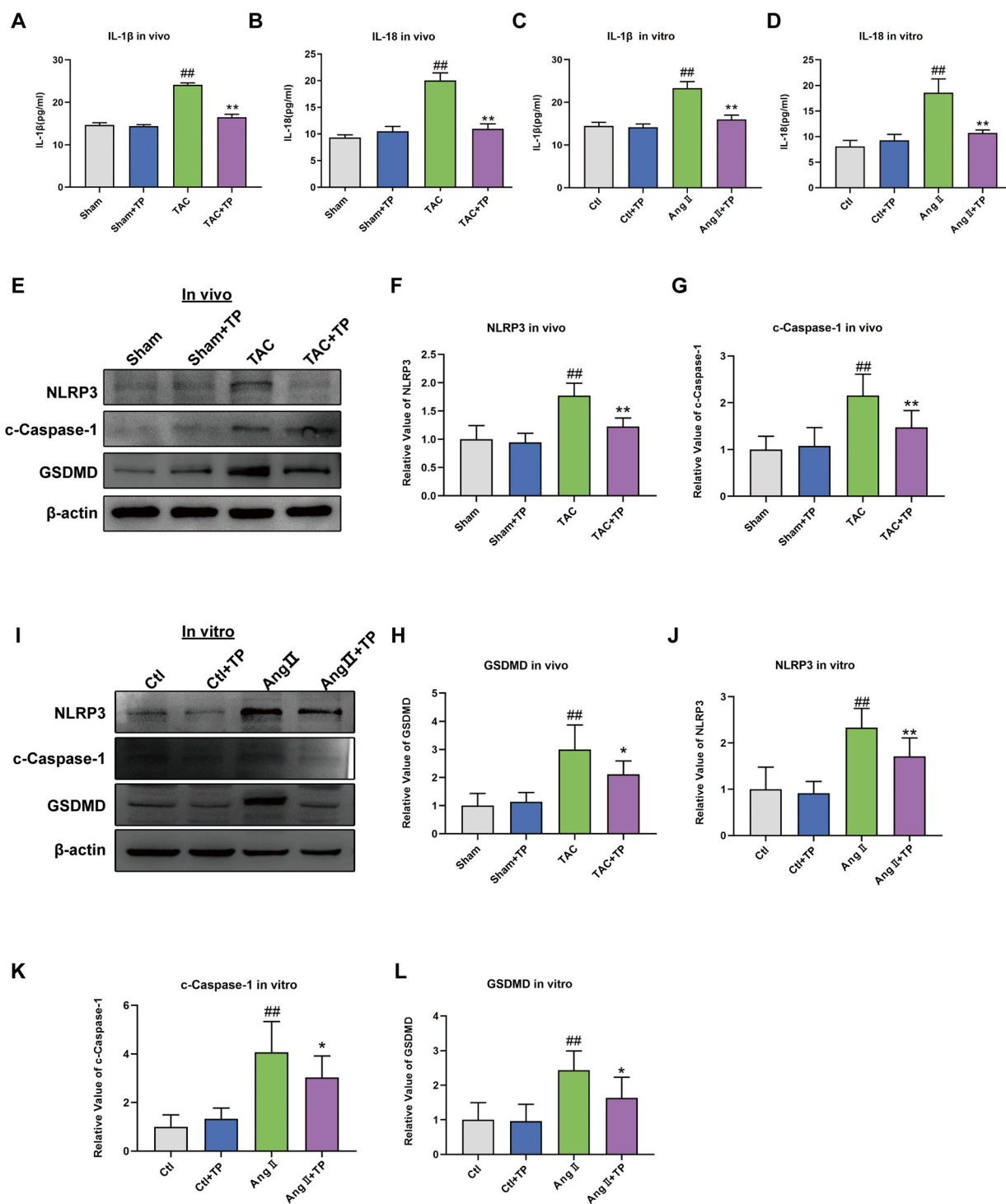
Fig. 3. TP inhibits pyroptosis in cardiac remodeling models. (A–B) The concentrations of IL-1β and IL-18 in serum (*n* = 3). **(C–D)** The concentrations of IL-1β and IL-18 in HL-1 cardiomyocytes (n = 3). **(E–H)** Western blot analysis of NLRP3, cleaved Caspase-1 and GSDMD protein expression in mouse heart tissue (*n* = 6). **(I–L)** Western blot analysis of NLRP3, cleaved Caspase-1 and GSDMD protein expression in HL-1 cardiomyocytes (n = 6). All the values are presented as mean ± SD. [#]P < 0.05, [##]P < 0.01 compared with Sham or Ctl group; *P < 0.05, **P < 0.01 compared with TAC or AngII group. The original blots were provided in supplementary data as Supplementary Fig. S2.
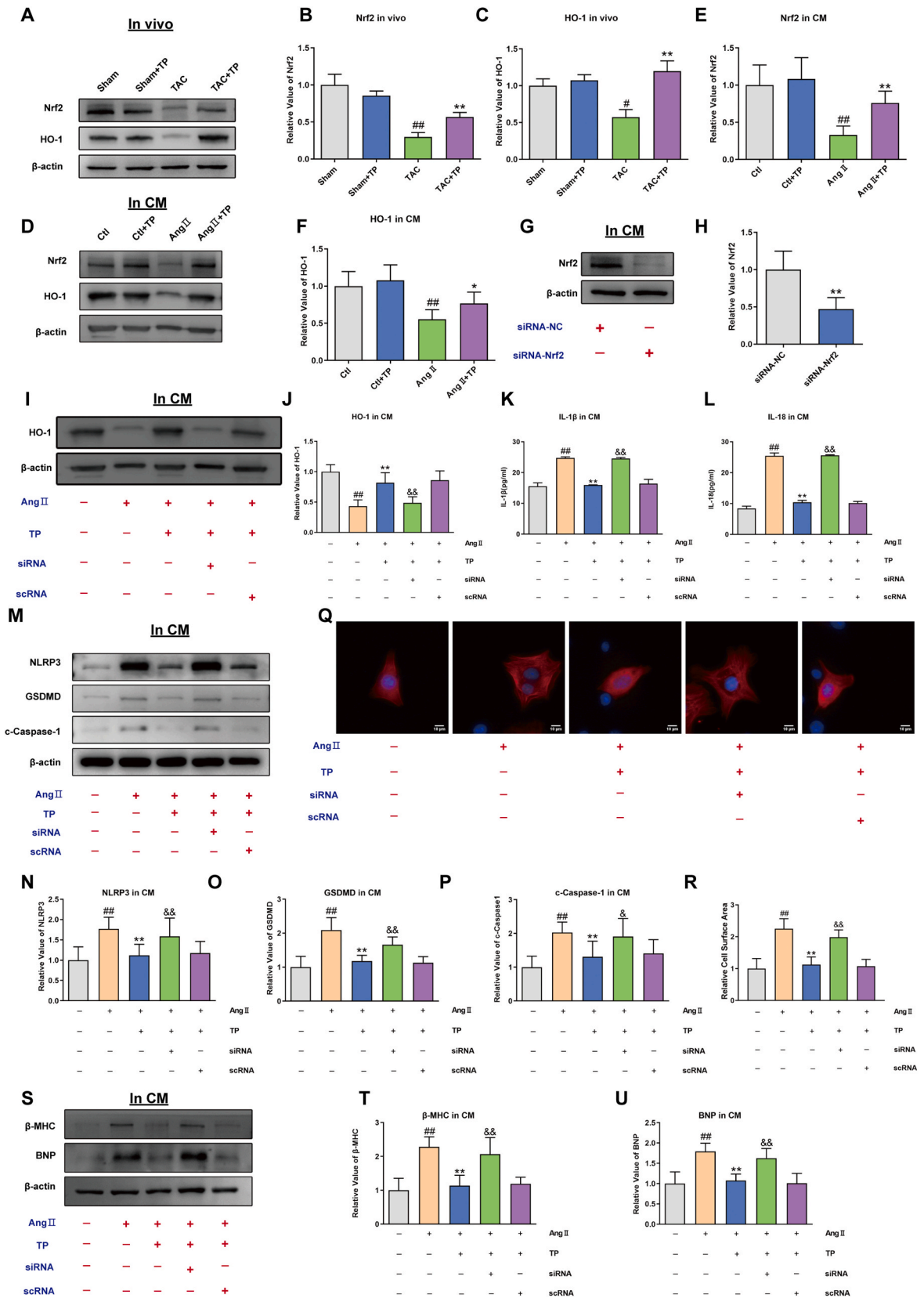
(caption on next page)

Fig. 4. TP suppresses pyroptosis via activating Nrf2/HO-1 pathway (**A**–**C**) Western blot analysis of Nrf2 and HO-1 protein expression in mouse heart tissue ($n = 6$). (**D**–**F**) Western blot analysis of Nrf2 and HO-1 in HL-1 cardiomyocytes ($n = 6$). (**G**–**H**) Western blot analysis of Nrf2 expression in the presence or absence of Nrf2 siRNA in HL-1 cardiomyocytes ($n = 6$). (**I**–**J**) HO-1 expression elicited by AngII in the presence or absence of Nrf2 siRNA in HL-1 cardiomyocytes ($n = 6$). (**K**–**L**) The concentrations of IL-1β and IL-18 in the presence or absence of Nrf2 siRNA in HL-1 cardiomyocytes ($n = 3$). (**M**–**P**) Western blot analysis of NLRP3, cleaved Caspase-1 and GSDMD expression in the presence or absence of Nrf2 siRNA in HL-1 cardiomyocytes ($n = 6$). (**Q**) Representative immunofluorescent staining of the cardiomyocytes (HL-1, α-actinin, red) and nuclei (DAPI, blue) elicited by AngII in the presence or absence of Nrf2 siRNA in HL-1 cardiomyocytes. Scale bar: 10 μm (n = 6). (**R**) Relative surface area of HL-1 cardiomyocytes (n = 6). (**S**–**U**) Western blot analysis of β-MHC and BNP expression in the presence or absence of Nrf2 siRNA in HL-1 cardiomyocytes (n = 6). All the values are presented as mean ± SD. [#]P < 0.05, [##]P < 0.01 compared with Ctl group; *P < 0.05, **P < 0.01 compared with siRNA-NC group or AngII group; [&]P < 0.05, [&&]P < 0.01 compared with AngII+TP + scRNA group. The original blots were provided in supplementary data as Supplementary Fig. S3.

(Fig. 6I-L). These findings further support the hypothesis that TP protects against TGF-β1-induced EndMT changes by activating the Nrf2 pathway.

3.6. TP activates Nrf2 signaling by decreasing ubiquitin-proteasome degradation of Nrf2

The targets of the TP were predicted using PharmMapper databases according to the 3-dimensional chemical structures (Fig. 7A). A total 278 predictive targets were identified, and ultimately, 111 official symbols of TP related targets for limiting to "*Mus musculus*" were obtained in the UniProt database after filtering by z-score >0. A large number of studies have shown that Nrf2 binds to the DGR domain of KEAP1 through its ETGE and DLG motif in the cytoplasm, which results in its degradation by the proteasome [40]. Therefore, we predict TP promoted Nrf2 activation by accelerated Keap1 protein degradation. Among 135 TP related targets, USP14, a proteasome-associated deubiquitinating enzyme, aroused our great interest. The results found that TP inhibited USP14 and KEAP1 expression *in vivo* (Fig. 7B–D) and *in vitro* (Fig. 7E–J). To further determine whether inhibition of USP14 activates the Keap1/Nrf2 signaling pathway, the changes in Keap1 and Nrf2 expression under the silencing USP14 were evaluated (Fig. 7K-N). Keap1 expression was dramatically elevated in the AngII treated cardiomyocytes and TGF-β1 treated endothelial cells; Keap1 interacted with Nrf2 to inactivate it. However, after the silencing USP14, the tendency was reversed. Keap1 expression was reduced, whereas Nrf2 expression was increased (Fig. 7O–T). It is supposed that USP14 may inhibited Keap1 protein degradation and reduced Nrf2 releases to translocate into the nucleus. To investigate the relationship between Keap1 and USP14, co-immunoprecipitation (Co-IP) experiments was performed. Western blotting showed that Keap1 interacts with USP14 (Fig. 7U–V).

These results reinforce our hypothesis that TP may promote Nrf2 activation by accelerating Keap1 protein degradation through inhibiting USP14. Additionally, the results showed that the interaction between Keap1 and USP14 plays a key role in regulating the Keap1/Nrf2 pathway.

4. Discussion

When the heart is subjected to chronic pressure overload, it triggers a cascade of cellular and molecular changes, including cardiomyocyte pyroptosis, endothelial-mesenchymal transition, and inflammatory responses [41]. These changes ultimately lead to cardiac remodeling and subsequent heart failure. However, the underlying molecular mechanisms and therapeutic strategies remain incompletely understood. In this study, it is the first time to present the potential effects of TP on molecular/cellular cardiac events and ventricular dysfunction during pressure overload via the USP14/Keap1/Nrf2 signal axis.

In this study, the protective effect of TP on cardiac remodeling using a TAC-induced mouse model (*in vivo*) and an Ang II/TGFβ1-induced mouse cardiomyocyte/HCAEC model (*in vitro*) were examined. The results demonstrate that after 4 weeks of TAC induction, there were apparent signs of cardiac remodeling and dysfunction. However, TP was found to attenuate the deleterious changes induced by pressure overload in cardiac remodeling in mice. This suggests that TP may have a significant role in the prevention of pressure overload-induced cardiac remodeling and could potentially be a promising therapeutic agent.

Cardiac hypertrophy is known to be a feature of cardiac remodeling [42]. In subsequent experiments, we will further explore the mechanism of TP inhibiting cardiac hypertrophy. Pyroptosis is a specific inflammatory form of programmed cell death characterized by Caspase-1 activation [43]. The role of pyroptosis in many cardiovascular diseases has been extensively studied in recent years. The findings indicate that after 4 weeks of TAC treatment in mice or 48 h of Ang II stimulation in mouse cardiomyocytes, a hypertrophic phenotype associated with cardiomyocyte pyroptosis is induced, suggesting that excessive myocardial pyroptosis may be involved in the development of cardiac hypertrophy. Interestingly, TP significantly reduced pyroptosis-positive cells in both hypertrophic models. Therefore, we hypothesized that TP prevents cardiac hypertrophy by inhibiting excessive cardiomyocyte pyroptosis. In order to confirm the link between TP and cardiomyocyte pyroptosis, related pyroptosis-promoting proteins and regulators were detected. The results showed that IL-1β and IL-18 levels were upregulated and the expression of cleaved Caspase-1, NLRP3 and GSDMD was increased. This effect can be reversed by treatment with triptolide. These results suggest that cardiomyocytes pyroptosis was induced and the therapeutic effect of TP on cardiac hypertrophy may be related to the inhibition of cardiomyocyte pyroptosis.

Cardiac fibrosis is another important feature of cardiac remodeling, which can lead to cardiac dysfunction and heart failure. In the current study, TP inhibited ECM deposition during cardiac remodeling in mice. At the same time, the expressions of Col I and III, the markers of cardiac fibrosis, were significantly decreased in the TP treatment group.

In the following experiment, we will elucidate the molecular mechanism of TP inhibiting cardiac fibrosis. Emerging evidence
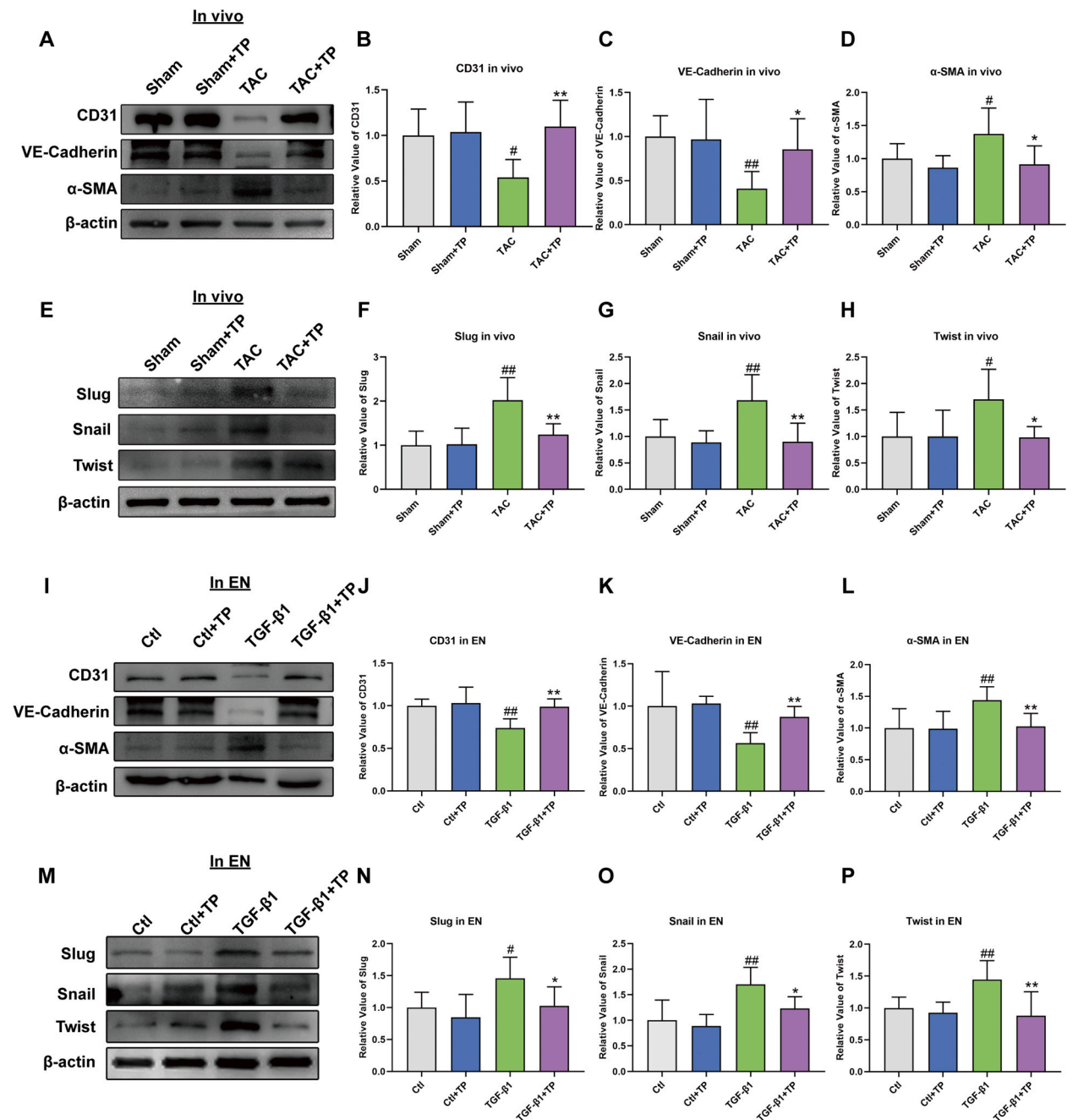
Fig. 5. TP inhibits EndMT in cardiac remodeling models. (A–D) Western blot analysis of CD31, VE-Cadherin and α-SMA protein expression in mouse heart tissue (n = 6). **(E–H)** Western blot analysis of Slug, Snail and Twist protein expression in mouse heart tissue (n = 6). **(I–L)** Western blot analysis of CD31, VE-Cadherin and α-SMA in EN (HCAEC) (n = 6). **(M–P)** Western blot analysis of Slug, Snail and Twist in EN (HCAEC) (n = 6). All the values are presented as mean ± SD. $^{\#}$P < 0.05, $^{\#\#}$P < 0.01 compared with Sham or Ctl group; *P < 0.05, **P < 0.01 compared with TAC or TGF-β1 group. The original blots were provided in supplementary data as Supplementary Fig. S4.

suggests that EndMT plays an important role in cardiac fibrosis [29,32]. In the results, TP treatment significantly upregulated the expression of the endothelial cell markers CD31, VE-Cadherin and decreased the mesenchymal cell marker α-SMA *in vivo* and *in vitro*.

Snail, Slug, and Twist have been reported to be the main transcription factors regulating EndMT [22]. The results showed that TP could inhibit the expression of Snail, Slug and Twist *in vitro* and *in vivo*. Therefore, TP can inhibit EndMT in endothelial cells by regulating key transcription factors.

Nrf2 is a transcription factor that activates the expression of cytoprotective genes, including HO-1, NQO1, and others [44]. Emerging studies have suggested that activation of the Nrf2 signaling pathway plays a critical role in inhibiting pyroptosis and EndMT
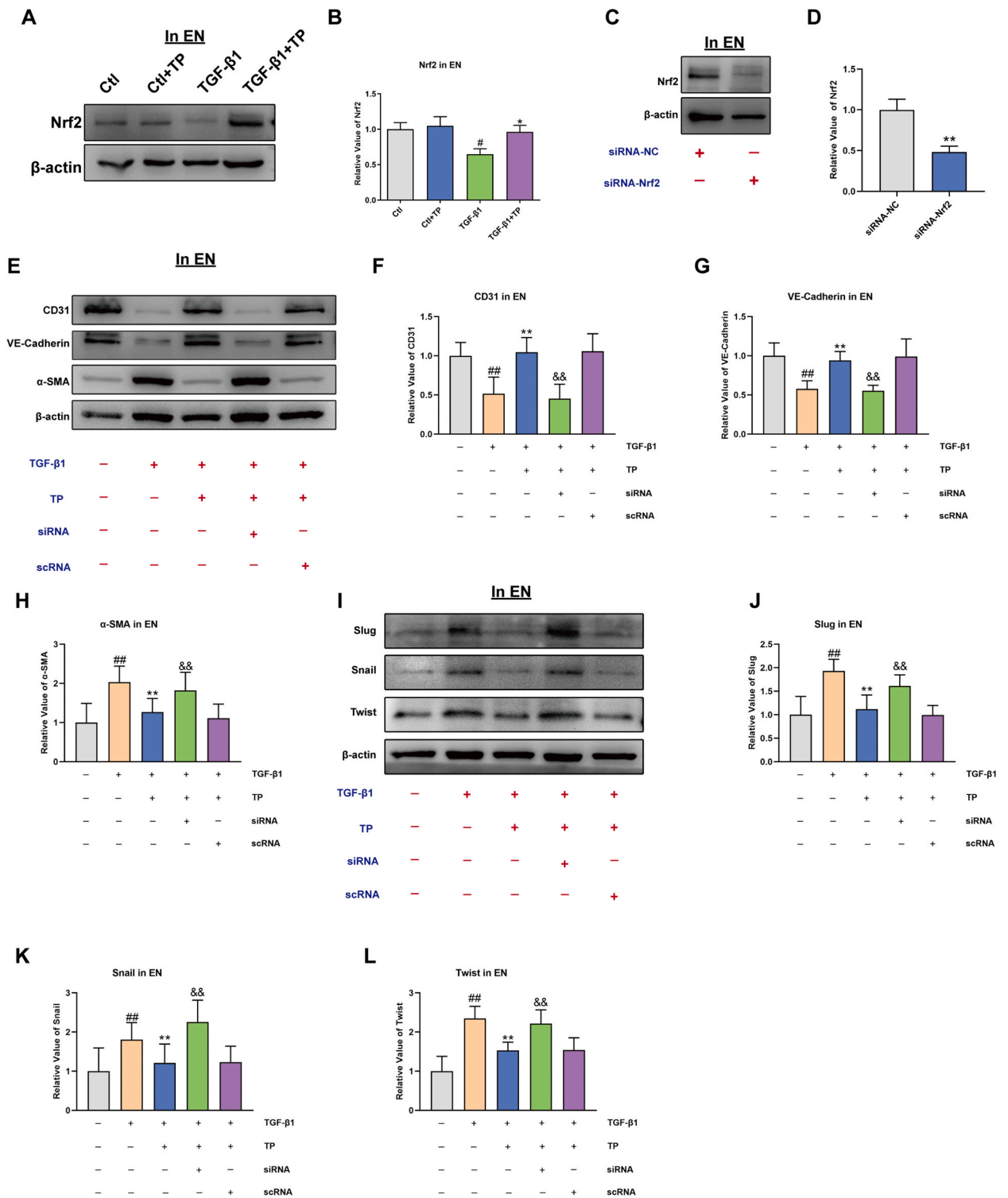
Fig. 6. TP inhibits EndMT via Nrf2 pathway. (A–B) Western blot analysis of Nrf2 in EN (HCAEC) ($n = 6$). **(C–D)** Western blot analysis of Nrf2 expression in the presence or absence of Nrf2 siRNA in EN (HCAEC) **($n = 6$)**. **(E–H)** CD31, VE-Cadherin and α-SMA expression elicited by TGF-β1 in the presence or absence of Nrf2 siRNA in EN (HCAEC) (n = 6) **(I–L)** Slug, Snail and Twist expression elicited by TGF-β1 in the presence or absence of Nrf2 siRNA in EN (HCAEC) (n = 6). All the values are presented as mean ± SD. [#]$P < 0.05$, [##]$P < 0.01$ compared with Ctl group; *P < 0.05, **P < 0.01 compared with siRNA-NC group or TGF-β1 group; [&]$P < 0.05$, [&&]$P < 0.01$ compared with TGF-β1+TP + scRNA group. The original blots were provided in supplementary data as Supplementary Fig. S5.
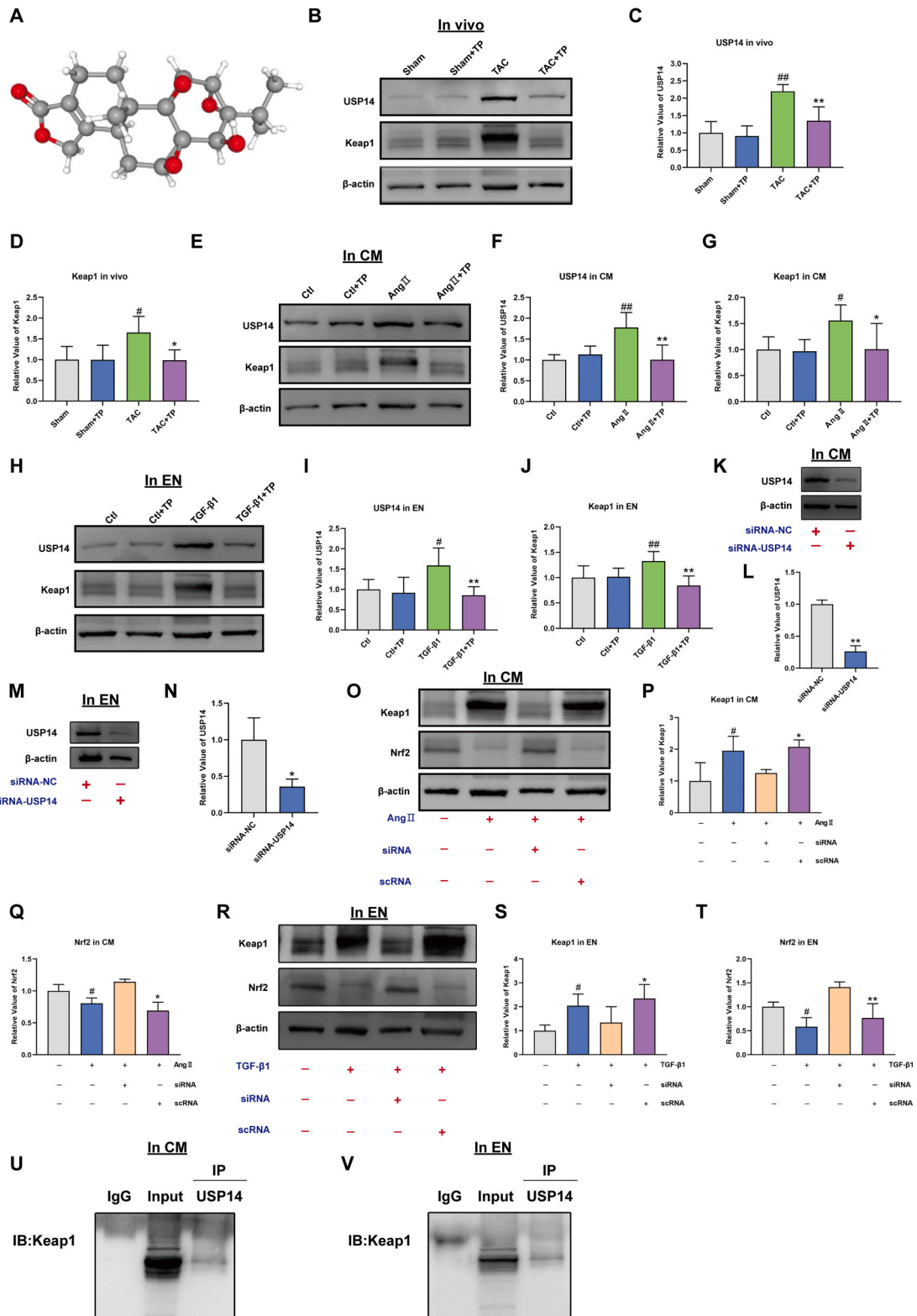
Fig. 7. Triptolide activates Nrf2 signaling by decreasing ubiquitin-proteasome degradation of Nrf2. (A) 3-dimensional chemical structures of Triptolide. **(B–D)** Western blot analysis of USP14 and Keap1 in mouse heart tissue (n = 6). **(E–G)** Western blot analysis of USP14 and Keap1 in mouse cardiomyocytes (HL-1) (n = 6). **(H–J)** Western blot analysis of USP14 and Keap1 in EN (HCAEC) (n = 6). **(K–L)** Western blot analysis of USP14 expression in the presence or absence of USP14 siRNA in mouse cardiomyocytes (HL-1) (*n* = 6). **(M–N)** Western blot analysis of USP14

expression in the presence or absence of USP14 siRNA in EN (HCAEC) ($n = 6$). **(O–Q)** Keap1 and Nrf2 expression elicited by AngII in the presence or absence of USP14 siRNA in mouse cardiomyocytes (HL-1) ($n = 3$). **(R–T)** Keap1 and Nrf2 expression elicited by AngII in the presence or absence of USP14 siRNA in EN (HCAEC) ($n = 3$). **(U and V)** The mouse cardiomyocytes (HL-1) and EN (HCAEC) was taken for Co-IP. Western blotting showed that Keap1 interacts with USP14. The original blots were provided in supplementary data as Supplementary Fig. S6.

[39,45]. In present study, the results indicated that the expressions of Nrf2 protein were decreased in TAC mice hearts, cardiomyocytes treated with Ang II, and endothelial cells treated with TGFβ1. However, these effects could be abrogated by TP. These data suggest that TP might suppress cardiac remodeling through the Nrf2 signaling pathway.

To further confirm the protective effect of TP through the Nrf2 signaling pathway, siRNA Nrf2 was transfected to mouse AngII-induced cardiomyocytes and endothelial cells treated with TGF-β1. TP treatment significantly reduced cardiomyocyte surface area and BNP and β-MHC expression, whereas Nrf2 silencing reversed these effects despite TP treatment. Furthermore, the results show that Nrf2 silencing increases IL-1β, IL-18, cleaved-Caspase-1, NLRP3 and GSDMD despite the presence of TP. Meanwhile, the inhibitory effect of TP on EndMT was reversed by Nrf2 silencing. These results suggest that TP inhibits cardiomyocyte pyroptosis and endothelial EndMT by activating Nrf2 signaling, thereby preventing cardiac remodeling.

The ubiquitin-proteasome system (UPS) is considered the primary protein degradation pathway in mammalian cells, responsible for the degradation of a significant number of proteins. Protecting cells from misfolded or damaged proteins is one of the essential functions of UPS [46]. In this study, the abnormal increase in Keap1 protein during cardiac remodeling was linked to UPS dysfunction, as evidenced by Keap1 protein restoration following USP14 silencing. The decrease in Nrf2 release, which correlates with the inhibition of pyroptosis and EndMT, may be attributable to the reduced Keap1 protein levels.

In present research, the results revealed a connection between USP14 and Keap1. It was found that USP14 interacts with Keap1 through the proteasomal degradation pathway, which leads to the stabilization of the abnormally elevated Keap1 protein by degradation via the proteasome pathway. This stabilization of Keap1 may be correlated with the reduced release of Nrf2 into the nucleus, resulting in an inhibitory impact on pyroptosis and EndMT. Additionally, the PharMapper database indicated that USP14 was the target of triptolide. It was discovered that triptolide had an inhibitory effect on USP14 and Keap1 expression while promoting Nrf2 expression.

5. Conclusion

In summary, the present research indicates that TP acts as an important regulator of cardiac remodeling. The protective function of TP is involved the inhibition of cardiomyocyte pyroptosis and endothelial cell EndMT through the suppression of the USP14/Keap1/Nrf2 axis, and in the future, TP therapy may be utilized as a therapeutic approach to address cardiac remodeling.

Data availability statement

Data will be made available on request.

Funding statement

CRediT authorship contribution statement

Lina Ba: Writing – original draft, Methodology, Investigation, Data curation, Conceptualization. **Mingyao E:** Writing – review & editing, Investigation. **Ruixuan Wang:** Investigation. **Nan Wu:** Software, Data curation. **Rui Wang:** Formal analysis, Data curation. **Renling Liu:** Investigation. **Xiang Feng:** Investigation. **Hanping Qi:** Writing – review & editing, Supervision. **Hongli Sun:** Writing – review & editing, Supervision. **Guofen Qiao:** Writing – review & editing, Supervision, Resources, Formal analysis, Data curation, Conceptualization.

Declaration of competing interest

The authors declare that they have no known competing financial interests or personal relationships that could have appeared to influence the work reported in this paper.

Appendix A. Supplementary data

Supplementary data to this article can be found online at https://doi.org/10.1016/j.heliyon.2024.e24010.

References

[1] J. Francisco, J. Guan, Y. Zhang, Y. Nakada, S. Mareedu, E. Sung, C.M. Hu, S. Oka, P. Zhai, J. Sadoshima, D.P. Del Re, Suppression of myeloid YAP antagonizes adverse cardiac remodeling during pressure overload stress, J. Mol. Cell. Cardiol. 181 (2023) 1–14, https://doi.org/10.1016/j.yjmcc.2023.05.004.

[2] S. Ye, H. Huang, X. Han, W. Luo, L. Wu, Y. Ye, Y. Gong, X. Zhao, W. Huang, Y. Wang, X. Long, G. Fu, G. Liang, Dectin-1 acts as a non-classical receptor of Ang II to induce cardiac remodeling, Circ. Res. 132 (6) (2023) 707–722, https://doi.org/10.1161/CIRCRESAHA.122.322259.

[3] L.E. Dorn, W. Lawrence, J.M. Petrosino, X. Xu, T.J. Hund, B.A. Whitson, M.S. Stratton, P.M.L. Janssen, P.J. Mohler, A. Schlosser, G.L. Sorensen, F. Accornero, Microfibrillar-associated protein 4 regulates stress-induced cardiac remodeling, Circ. Res. 128 (6) (2021) 723–737, https://doi.org/10.1161/CIRCRESAHA.120.317146.

[4] C. Lerchenmuller, C.P. Rabolli, A. Yeri, R. Kitchen, A.M. Salvador, L.X. Liu, O. Ziegler, K. Danielson, C. Platt, R. Shah, F. Damilano, P. Kundu, E. Riechert, H. A. Katus, J.E. Saffitz, H. Keshishian, S.A. Carr, V.J. Bezzerides, S. Das, A. Rosenzweig, CITED4 protects against adverse remodeling in response to physiological and pathological stress, Circ. Res. 127 (5) (2020) 631–646, https://doi.org/10.1161/CIRCRESAHA.119.315881.

[5] Y.P. Xie, S. Lai, Q.Y. Lin, X. Xie, J.W. Liao, H.X. Wang, C. Tian, H.H. Li, CDC20 regulates cardiac hypertrophy via targeting LC3-dependent autophagy, Theranostics 8 (21) (2018) 5995–6007, https://doi.org/10.7150/thno.27706.

[6] L. Zhao, Z. Lan, L. Peng, L. Wan, D. Liu, X. Tan, C. Tang, G. Chen, H. Liu, Triptolide promotes autophagy to inhibit mesangial cell proliferation in IgA nephropathy via the CARD9/p38 MAPK pathway, Cell Prolif. 55 (9) (2022) e13278, https://doi.org/10.1111/cpr.13278.

[7] H. Zhu, S. Tong, C. Yan, A. Zhou, M. Wang, C. Li, Triptolide attenuates LPS-induced activation of RAW 264.7 macrophages by inducing M1-to-M2 repolarization via the mTOR/STAT3 signaling, Immunopharmacol. Immunotoxicol. 44 (6) (2022) 894–901, https://doi.org/10.1080/08923973.2022.2093738.

[8] L. Li, C. Wang, Z. Qiu, D. Deng, X. Chen, Q. Wang, Y. Meng, B. Zhang, G. Zheng, J. Hu, Triptolide inhibits intrahepatic cholangiocarcinoma growth by suppressing glycolysis via the AKT/mTOR pathway, Phytomedicine 109 (2023) 154575, https://doi.org/10.1016/j.phymed.2022.154575.

[9] Y. Xie, J. Ding, J. Gao, J. Zhang, S. Cen, J. Zhou, Triptolide reduces PD-L1 through the EGFR and IFN-gamma/IRF1 dual signaling pathways, Int. Immunopharm. 118 (2023) 109993, https://doi.org/10.1016/j.intimp.2023.109993.

[10] G. Liu, L. Wang, M. Tuerxunyiming, J. Xu, Z. Wu, W. Wang, H. Liu, L. Lin, Q. Liu, Triptolide ameliorates osteoarthritis by regulating nuclear factor kappa B-mediated inflammatory response, J. Pharm. Pharmacol. (2022), https://doi.org/10.1093/jpp/rgab182.

[11] A. Xu, R. Yang, M. Zhang, X. Wang, Y. Di, B. Jiang, Y. Di, Z. Zhou, L. Zhou, Macrophage targeted triptolide micelles capable of cGAS-STING pathway inhibition for rheumatoid arthritis treatment, J. Drug Target. 30 (9) (2022) 961–972, https://doi.org/10.1080/1061186X.2022.2070173.

[12] H. He, A. Takahashi, T. Mukai, A. Hori, M. Narita, A. Tojo, T. Yang, T. Nagamura-Inoue, The immunomodulatory effect of triptolide on mesenchymal stromal cells, Front. Immunol. 12 (2021) 686356, https://doi.org/10.3389/fimmu.2021.686356.

[13] K. Lai, Y. Li, L. Li, Y. Gong, C. Huang, Y. Zhang, L. Cheng, F. Xu, H. Zhao, C. Li, X. Zhong, C. Jin, Intravitreal injection of triptolide attenuates subretinal fibrosis in laser-induced murine model, Phytomedicine 93 (2021) 153747, https://doi.org/10.1016/j.phymed.2021.153747.

[14] B. Yang, P. Yan, G.Z. Yang, H.L. Cao, F. Wang, B. Li, Triptolide reduces ischemia/reperfusion injury in rats and H9C2 cells via inhibition of NF-kappaB, ROS and the ERK1/2 pathway, Int. J. Mol. Med. 41 (6) (2018) 3127–3136, https://doi.org/10.3892/ijmm.2018.3537.

[15] Y. Xi, Y. Zhang, J. Pan, S. Chen, S. Lu, F. Shen, Z. Huang, Triptolide dysregulates glucose uptake via inhibition of IKKbeta-NF-kappaB pathway by p53 activation in cardiomyocytes, Toxicol. Lett. 318 (2020) 1–11, https://doi.org/10.1016/j.toxlet.2019.10.001.

[16] X.C. Pan, Y.L. Xiong, J.H. Hong, Y. Liu, Y.Y. Cen, T. Liu, Q.F. Yang, H. Tao, Y.N. Li, H.G. Zhang, Cardiomyocytic FoxP3 is involved in Parkin-mediated mitophagy during cardiac remodeling and the regulatory role of triptolide, Theranostics 12 (5) (2022) 2483–2501, https://doi.org/10.7150/thno.71102.

[17] L. Li, J. Qi, H. Tao, L. Wang, L. Wang, N. Wang, Q. Huang, Protective effect of the total flavonoids from Clinopodium chinense against LPS-induced mice endometritis by inhibiting NLRP3 inflammasome-mediated pyroptosis, J. Ethnopharmacol. 312 (2023) 116489, https://doi.org/10.1016/j.jep.2023.116489.

[18] N. Zhou, Y. Chen, J. Wang, R. An, H. Cai, S. Liu, L. Yao, Y. Tang, L. Chen, J. Du, TgMIF promotes hepatocyte pyroptosis and recruitment of proinflammatory macrophages during severe liver injury in acute Toxoplasmosis, J. Infect. Dis. 227 (12) (2023) 1417–1427, https://doi.org/10.1093/infdis/jiac422.

[19] H. Luo, X. Liu, H. Liu, Y. Wang, K. Xu, J. Li, M. Liu, J. Guo, X. Qin, ACT001 Ameliorates ionizing radiation-induced lung injury by inhibiting NLRP3 inflammasome pathway, Biomed. Pharmacother. 163 (2023) 114808, https://doi.org/10.1016/j.biopha.2023.114808.

[20] C. Ding, X. Yang, S. Li, E. Zhang, X. Fan, L. Huang, Z. He, J. Sun, J. Ma, L. Zang, M. Zheng, Exploring the role of pyroptosis in shaping the tumor microenvironment of colorectal cancer by bulk and single-cell RNA sequencing, Cancer Cell Int. 23 (1) (2023) 95, https://doi.org/10.1186/s12935-023-02897-8.

[21] R. Chai, W. Xue, S. Shi, Y. Zhou, Y. Du, Y. Li, Q. Song, H. Wu, Y. Hu, Cardiac remodeling in heart failure: role of pyroptosis and its therapeutic implications, Front Cardiovasc Med 9 (2022) 870924, https://doi.org/10.3389/fcvm.2022.870924.

[22] B. Wang, Z. Wu, Y. Wu, L. Zha, X. Zhang, Y. Yan, Y. Xie, MFGE8 is down-regulated in cardiac fibrosis and attenuates endothelial-mesenchymal transition through Smad2/3-Snail signalling pathway, J. Cell Mol. Med. 24 (21) (2020) 12799–12812, https://doi.org/10.1111/jcmm.15871.

[23] Z. Lei, F. Luan, X. Zhang, L. Peng, B. Li, X. Peng, Y. Liu, R. Liu, N. Zeng, Piperazine ferulate protects against cardiac ischemia/reperfusion injury in rat via the suppression of NLRP3 inflammasome activation and pyroptosis, Eur. J. Pharmacol. 920 (2022) 174856, https://doi.org/10.1016/j.ejphar.2022.174856.

[24] R. Yue, Z. Zheng, Y. Luo, X. Wang, M. Lv, D. Qin, Q. Tan, Y. Zhang, T. Wang, H. Hu, NLRP3-mediated pyroptosis aggravates pressure overload-induced cardiac hypertrophy, fibrosis, and dysfunction in mice: cardioprotective role of irisin, Cell Death Dis. 7 (1) (2021) 50, https://doi.org/10.1038/s41420-021-00434-y.

[25] F. Wang, Q. Liang, Y. Ma, M. Sun, T. Li, L. Lin, Z. Sun, J. Duan, Silica nanoparticles induce pyroptosis and cardiac hypertrophy via ROS/NLRP3/Caspase-1 pathway, Free Radic. Biol. Med. 182 (2022) 171–181, https://doi.org/10.1016/j.freeradbiomed.2022.02.027.

[26] B.L. Tang, Y. Liu, J.L. Zhang, M.L. Lu, H.X. Wang, Ginsenoside Rg1 ameliorates hypoxia-induced pulmonary arterial hypertension by inhibiting endothelial-to-mesenchymal transition and inflammation by regulating CCN1, Biomed. Pharmacother. 164 (2023) 114920, https://doi.org/10.1016/j.biopha.2023.114920.

[27] X. Sun, Y. Sun, P. Jiang, G. Qi, X. Chen, Crosstalk between endothelial cell-specific calpain inhibition and the endothelial-mesenchymal transition via the HSP90/Akt signaling pathway, Biomed. Pharmacother. 124 (2020) 109822, https://doi.org/10.1016/j.biopha.2020.109822.

[28] S. Kim, H. Lee, H. Moon, R. Kim, M. Kim, S. Jeong, H. Kim, S.H. Kim, S.S. Hwang, M.Y. Lee, J. Kim, B.W. Song, W. Chang, Epigallocatechin-3-Gallate attenuates myocardial dysfunction via inhibition of endothelial-to-mesenchymal transition, Antioxidants 12 (5) (2023), https://doi.org/10.3390/antiox12051059.

[29] J. Chen, J. Jia, L. Ma, B. Li, Q. Qin, J. Qian, J. Ge, Nur 77 deficiency exacerbates cardiac fibrosis after myocardial infarction by promoting endothelial-to-mesenchymal transition, J. Cell. Physiol. 236 (1) (2021) 495–506, https://doi.org/10.1002/jcp.29877.

[30] Y. Liu, L. Gao, X. Zhao, S. Guo, Y. Liu, R. Li, C. Liang, L. Li, J. Dong, L. Li, H. Yang, Saikosaponin A protects from pressure overload-induced cardiac fibrosis via inhibiting fibroblast activation or endothelial cell EndMT, Int. J. Biol. Sci. 14 (13) (2018) 1923–1934, https://doi.org/10.7150/ijbs.27022.

[31] G. Liang, S. Wang, J. Shao, Y.J. Jin, L. Xu, Y. Yan, S. Gunther, L. Wang, S. Offermanns, Tenascin-X mediates flow-induced suppression of EndMT and atherosclerosis, Circ. Res. 130 (11) (2022) 1647–1659, https://doi.org/10.1161/CIRCRESAHA.121.320694.

[32] E.M. Zeisberg, O. Tarnavski, M. Zeisberg, A.L. Dorfman, J.R. McMullen, E. Gustafsson, A. Chandraker, X. Yuan, W.T. Pu, A.B. Roberts, E.G. Neilson, M. H. Sayegh, S. Izumo, R. Kalluri, Endothelial-to-mesenchymal transition contributes to cardiac fibrosis, Nat. Med. 13 (8) (2007) 952–961, https://doi.org/10.1038/nm1613.

[33] Y. Liu, L. Gao, S. Guo, Y. Liu, X. Zhao, R. Li, X. Yan, Y. Li, S. Wang, X. Niu, L. Yao, Y. Zhang, L. Li, H. Yang, Kaempferol alleviates angiotensin II-induced cardiac dysfunction and interstitial fibrosis in mice, Cell. Physiol. Biochem. 43 (6) (2017) 2253–2263, https://doi.org/10.1159/000484304.

[34] L. Zhang, J. He, J. Wang, J. Liu, Z. Chen, B. Deng, L. Wei, H. Wu, B. Liang, H. Li, Y. Huang, L. Lu, Z. Yang, S. Xian, L. Wang, Knockout RAGE alleviates cardiac fibrosis through repressing endothelial-to-mesenchymal transition (EndMT) mediated by autophagy, Cell Death Dis. 12 (5) (2021) 470, https://doi.org/10.1038/s41419-021-03750-4.

[35] S.C. Harper, J. Johnson, G. Borghetti, H. Zhao, T. Wang, M. Wallner, H. Kubo, E.A. Feldsott, Y. Yang, Y. Joo, X. Gou, A.K. Sabri, P. Gupta, M. Myzithras, A. Khalil, M. Franti, S.R. Houser, GDF11 decreases pressure overload-induced hypertrophy, but can cause severe Cachexia and Premature death, Circ. Res. 123 (11) (2018) 1220–1231, https://doi.org/10.1161/CIRCRESAHA.118.312955.

[36] H. Qi, J. Ren, M. E, Q. Zhang, Y. Cao, L. Ba, C. Song, P. Shi, B. Fu, H. Sun, MiR-103 inhibiting cardiac hypertrophy through inactivation of myocardial cell autophagy via targeting TRPV3 channel in rat hearts, J. Cell Mol. Med. 23 (3) (2019) 1926–1939, https://doi.org/10.1111/jcmm.14095.

[37] S. Ruhl, K. Shkarina, B. Demarco, R. Heilig, J.C. Santos, P. Broz, ESCRT-dependent membrane repair negatively regulates pyroptosis downstream of GSDMD activation, Science 362 (6417) (2018) 956–960, https://doi.org/10.1126/science.aar7607.

[38] H. Sabbineni, A. Verma, S. Artham, D. Anderson, O. Amaka, F. Liu, S.P. Narayanan, P.R. Somanath, Pharmacological inhibition of beta-catenin prevents EndMT in vitro and vascular remodeling in vivo resulting from endothelial Akt 1 suppression, Biochem. Pharmacol. 164 (2019) 205–215, https://doi.org/10.1016/j.bcp.2019.04.016.

[39] Y. Chen, T. Yuan, H. Zhang, Y. Yan, D. Wang, L. Fang, Y. Lu, G. Du, Activation of Nrf2 attenuates pulmonary vascular remodeling via inhibiting endothelial-to-mesenchymal transition: an insight from a plant polyphenol, Int. J. Biol. Sci. 13 (8) (2017) 1067–1081, https://doi.org/10.7150/ijbs.20316.

[40] S. Li, M. Shi, Y. Wang, Y. Xiao, D. Cai, F. Xiao, Keap1-Nrf2 pathway up-regulation via hydrogen sulfide mitigates polystyrene microplastics induced-hepatotoxic effects, J. Hazard Mater. 402 (2021) 123933, https://doi.org/10.1016/j.jhazmat.2020.123933.

[41] Q. Li, C. Li, A. Elnwasany, G. Sharma, Y.A. An, G. Zhang, W.M. Elhelaly, J. Lin, Y. Gong, G. Chen, M. Wang, S. Zhao, C. Dai, C.D. Smart, J. Liu, X. Luo, Y. Deng, L. Tan, S.J. Lv, S.M. Davidson, J.W. Locasale, P.L. Lorenzi, C.R. Malloy, T.G. Gillette, M.G. Vander Heiden, P.E. Scherer, L.I. Szweda, G. Fu, Z.V. Wang, PKM1 exerts critical roles in cardiac remodeling under pressure overload in the heart, Circulation 144 (9) (2021) 712–727, https://doi.org/10.1161/CIRCULATIONAHA.121.054885.

[42] M. Zhao, J. Zhang, Y. Xu, J. Liu, J. Ye, Z. Wang, D. Ye, Y. Feng, S. Xu, W. Pan, M. Wang, J. Wan, Selective inhibition of NLRP3 inflammasome reverses pressure overload-induced pathological cardiac remodeling by attenuating hypertrophy, fibrosis, and inflammation, Int. Immunopharm. 99 (2021) 108046, https://doi.org/10.1016/j.intimp.2021.108046.

[43] Y. Bai, X. Sun, Q. Chu, A. Li, Y. Qin, Y. Li, E. Yue, H. Wang, G. Li, S.M. Zahra, C. Dong, Y. Jiang, Caspase-1 regulate AngII-induced cardiomyocyte hypertrophy via upregulation of IL-1 beta, Biosci. Rep. 38 (2) (2018), https://doi.org/10.1042/BSR20171438.

[44] F. Szepanowski, D.M. Donaldson, H.P. Hartung, A.K. Mausberg, C. Kleinschnitz, B.C. Kieseier, M. Stettner, Dimethyl fumarate accelerates peripheral nerve regeneration via activation of the anti-inflammatory and cytoprotective Nrf2/HO-1 signaling pathway, Acta Neuropathol. 133 (3) (2017) 489–491, https://doi.org/10.1007/s00401-017-1676-z.

[45] Q. Hu, T. Zhang, L. Yi, X. Zhou, M. Mi, Dihydromyricetin inhibits NLRP3 inflammasome-dependent pyroptosis by activating the Nrf2 signaling pathway in vascular endothelial cells, Biofactors 44 (2) (2018) 123–136, https://doi.org/10.1002/biof.1395.

[46] T. Ravid, M. Hochstrasser, Diversity of degradation signals in the ubiquitin-proteasome system, Nat. Rev. Mol. Cell Biol. 9 (9) (2008) 679–690, https://doi.org/10.1038/nrm2468.